The Kinetic Energy Pauli Enhancement Factor and Its Role in Determining the Shell Structure of Atoms and Molecules

Ludena, Eduardo V.; Arroyo, Dario; Salazar, Edison X.; Vallejo, Jorge

Published in:
NOVEL ELECTRONIC STRUCTURE THEORY: GENERAL INNOVATIONS AND STRONGLY CORRELATED SYSTEMS

DOI:
10.1016/bs.aiq.2017.05.002

CHAPTER THREE

The Kinetic Energy Pauli Enhancement Factor and Its Role in Determining the Shell Structure of Atoms and Molecules

Eduardo V. Ludeña*,†,1, Darío Arroyo*, Edison X. Salazar‡, Jorge Vallejo*

*Center of Nanotechnology Research and Development, CIDNA, Escuela Superior Politécnica del Litoral, ESPOL, Guayaquil, Ecuador
†Centro de Química, Instituto Venezolano de Investigaciones Científicas, IVIC, Caracas, Venezuela
‡Theoretical Chemistry, Zernike Institute for Advanced Materials, University of Groningen, Groningen, The Netherlands
[1]Corresponding author: e-mail address: popluabe@yahoo.es

Contents

Abstract

We deal with different representations of the noninteracting kinetic energy functional for the purpose of examining their effect upon the generation of shell structure in atoms. We decompose the noninteracting functional into a Weizsacker term plus a Pauli term where the latter is written as a product of the Thomas–Fermi $\rho^{5/3}(r)$ times the Pauli enhancement factor $F_p[\rho]$. We examine the behavior of $F_p[\rho]$ when it is given in terms of a Hartree–Fock orbital representation, of density-dependent orbitals generated through local-scaling transformations, and of the Liu–Parr power series

Advances in Quantum Chemistry, Volume 76
ISSN 0065-3276
https://doi.org/10.1016/bs.aiq.2017.05.002

expansion. In the latter, we compare the cases when the expansion coefficients have been expanded in an all-shell vs a shell-by-shell procedure. We apply these approximations to the aluminum atom. In particular, for this case, we examine in these different approximations, the role of the Pauli enhancement factor for the production of shell structure.

1. INTRODUCTION

In Kohn–Sham theory the introduction of the noninteracting kinetic energy functional T_s into the energy expression leads, upon functional differentiation, to a collection of one-particle equation whose solutions are the Kohn–Sham orbitals. This arises from the fact that $T_s[\{\phi_i\}_{i=1}^N]$ is naturally a functional of the occupied one-particle orbitals. However, one of the aims of density functional theory is to express the energy solely as a functional of the one particle density. Of course, the stumbling block is that as yet no satisfactory expression for $T_s[\rho]$ has been found, where $T_s[\rho]$ is a sufficiently accurate functional of only the one-electron density. Attaining this functional is essential for the development of, e.g., orbital-free molecular dynamics.

The shell structure of the electron distribution of atoms and molecules is an important ingredient in determining many chemical and physical properties of these many-electron systems. For example, the periodicity observed in the properties of the elements filling up the periodic table is linked to the formation of filled inner atomic shells and to the presence of valence electrons characterizing the groups or families. Although the existence of shell structure had been successfully hypothesized before the advent of quantum mechanics, its proper understanding and justification was only attained within its context. The shell structure arises from the Pauli exclusion principle and it is implicit already in the Schrödinger equation. It appears naturally in one-electron densities extracted from approximate theoretical calculations based on orbitals, whether they belong to the traditional quantum chemistry methods or to the DFT ones. Of course, its existence has also been confirmed by experimental work.

The aim of this chapter is to assess how well different representations of $T_s[\rho]$ meet with the requirement of reproducing shell structure. $T_s[\rho]$ can be exactly decomposed into the Weizsäcker plus the Pauli terms

$$T_s[\rho] = T_W[\rho] + T_P[\rho] \tag{1}$$

where

$$T_W[\rho] = (1/8)\int d^3\mathbf{r}|\nabla_{\mathbf{r}}\rho(\mathbf{r})|^2/\rho(\mathbf{r}) \quad (2)$$

$$T_P[\rho] = \int d^3\mathbf{r}\rho^{5/3}(\mathbf{r})F_P[\rho;\mathbf{r}] \quad (3)$$

Bearing in mind that $T_W[\rho]$ is related to the Fisher information entropy,[1,2] which is a local term,[3,4] shell structure may be ascribed to the behavior of the Pauli enhancement factor $F_P[\rho;\mathbf{r}]$, a nonlocal term.[5] For this reason, we examine the aptness of various representations of the Pauli enhancement factor to describe shell structure of atoms. We consider an orbital approximation, based on the Hartree–Fock orbitals of Clementi–Roetti. We also examine the exact implicit functional for $F_P[\rho;\mathbf{r}]$ generated by means of local-scaling transformations. Finally, we examine the Liu–Parr power series approximation.

In Section 2 we discuss the development of shell structure and Pauli potential concepts. In Section 3 we present results showing the relationship between the Pauli enhancement term and shell structure in atoms. Finally, in Section 4 we present some conclusions.

2. THE CONCEPTS OF SHELL STRUCTURE AND THE PAULI POTENTIAL

2.1 Shell Structure

In what follows we briefly outline, somewhat chronologically, the development of some of the ideas and experimental facts relating charge density to shell structure.

In 1927, Pauling[6] proposed a view of many-electron atoms in terms of electrons which filled atomic shells according to the Pauli exclusion principle.[7,8] In these early years in the development of quantum mechanics only the hydrogen atom had been solved by Schrödinger[9] and thus Pauling's proposal was somewhat revolutionary. However, assuming electron shells in atoms existed had previously been adopted by Unsöld for the interpretation of X-ray spectra.[10] The concentration of electronic charge in shells effectively shielded the positive charge in the nucleus and allowed treatment of an individual electron placed outside these shells as an electron in a hydrogen-like atom having a screened nuclear potential. This idea was further developed by Slater[11] with the introduction of atomic shielding constants.

For a spherically symmetrical atom $D(r)dr = 4\pi r^2\rho(r)dr$ is the average electron charge in a spherical shell of thickness dr. This quantity shows charge concentration and depletion. Experimental evidence of the existence of shell structure was obtained by reproducing the radial distribution $D(r)$ of atoms from electron diffraction data.[12] On the other hand, the density $\rho(r)$ decreases monotonically with r and does not present shell structure traits.[13,14] A model based on piece-wise exponentially decreasing densities was applied to atoms by Wang and Parr.[15] The asymptotic behavior of $\rho(r)$ at the nucleus and at infinity has been determined by Hoffmann-Ostenhof et al.[16,17] The electron one-particle density has also been extracted from single-crystal X-ray diffraction data using multipole expansions around the ionic centers.[18] Sagar et al. in 1988 using Hartree–Fock orbitals for atoms showed that the maxima in $D(r)$ correlate well with the shell radii from the Bohr–Schrödinger theory of an atom.[19] They also were able to relate the potential $\nabla^2\rho^{1/2}/(2\rho^{1/2})$ to the shell structure in atoms when $\rho(r)$ is obtained from the Clementi–Roetti HF orbitals.[20]

The convexity of the atomic charge distribution was shown to hold for some but not all atoms with $Z \leq 54$.[21] This result was extended by Esquivel et al. to show also the nonconvexity of ρ from Xe to U.[22] Moreover, the concept of pseudo-convexity has been used to define the general structural property of atomic densities as this concept embodies all the structural features empirically attributed to ρ.[23]

Kohout et al. were able to show that the quantity $-|\nabla\rho(r)|/\rho(r)$ is sufficient to determine the whole shell structure of atoms.[24] Schmider et al. have found that there exists a correlation between the extremal points and the roots of the Laplacian of the structure factor, namely, $\nabla^2 F(k)$, with Z.[25] The behavior of ideal shells (namely, those designed to hold the exact number of electrons required by the Aufbau principle) has been examined both in position and momentum space by Schmider et al.[26]

Parr and Zhou[27] propose "absolute hardness," as unifying concept for identifying shells and subshells in nuclei, atoms, molecules, and metallic clusters.

Another interesting line of work related to the properties of the one-particle density is based on Shannon information entropy of quantum-mechanical systems in central potentials.[28] Rigorous lower and upper bounds to the position and momentum Shannon entropies of many-electron systems have been determined.[29–31] The connection between Shannon information entropies and classical orthogonal polynomials has

been investigated.[32,33] The shell-filling properties of information measures have also been analyzed.[34]

Shell structure has also been found experimentally in quantum dots. In effect, by probing with far-infrared and capacitance spectroscopy it has been possible to distinguish, by their characteristic excitation frequencies, quantum dot Helium from quantum dot Lithium.[35] Shell structure has also been observed in sodium nanowires.[36]

Shell structure may also be related to the localization properties of electrons as described by the ELF function. Shell separation is related to the ELF's minima and the presence of shells to its maxima.[37] Another indicator of shell structure is provided by the average local electrostatic potential function, $V(r)/\rho(r)$; shell boundaries are found to be related to the successively increasing maxima of this indicator.[38] More recently, a localized electron detector, LED, has been advanced. Its aim is to show the three-dimensional structure of the different bonds identified by topological analysis of the density.[39–41] Other chemical indicators such as the curvature of the electron position uncertainty, described in terms of functions of the density have also recently been examined.

In a recent work, Finzel[42–47] has tackled the problem of incorporating the Pauli exclusion principle in the design of kinetic energy functionals for orbital-free treatments, through the concept of ideal atomic shells. This very simple idea captures, somehow, important characteristics that one should include in energy functionals expressed in terms of the one-particle density.

2.2 The Pauli Potential

The origin of the concept of the Pauli potential may be traced back to the work of March and Murray in 1966[48] who noticed that the potentials obtained as functional derivatives of the von Weizsäcker plus the Thomas–Fermi terms were insufficient to fully explain the behavior of electrons in finite metals. More directly, it arises from the Schrödinger equation for the square root of the density[49–51] where it takes the place of the local potential coming from the corrections to the Thomas–Fermi functional. The Pauli potential also emerges as an implicit functional of the one-particle density in the derivation carried out by Kryachko and Ludeña in 1992, in the context of local-scaling transformations, of the equations for the square root of the density.[52] It was shown in 1994 that the Pauli potential must satisfy the inequality $v_p(\rho, \mathbf{r}) \geq 0$.[53] The effect of harmonic confinement on the Pauli potential and its relation to the differential virial theorem has been examined by March.[54]

This same author has reviewed the concept of the Pauli potential emphasizing its importance in relation to density functional theory, DFT.[55]

The recent importance of the Pauli potential is related to the formulation of orbital-free molecular dynamics, OF-MD, where, in addition to the Kohn–Sham potential of the usual DFT, there arises also the Pauli potential from the noninteracting kinetic energy functional. Clearly, an OF-MD treatment of many-electron systems has the advantage over the traditional Kohn–Sham method that it does not rely on orbitals. The equations one has to deal with in OF-MD are related to the density or to its square root. However, these equations contain the Pauli potential as an additional term. For this reason, the proper representation of the Pauli potential becomes a crucial problem in this formalism. Recently, research has focussed on the conditions, such as the cusp condition, that this potential must satisfy.[56] The Pauli potential has also been investigated in the context of Natural Orbital Functional Theory.[57] More recently, the relation between the Pauli potential and shell structure has been investigated by Finzel.[44] In a very interesting recent work, differential equations for the Pauli potential have been advanced. Clearly, such an approach presents an alternative to the traditional Kohn–Sham orbital theory.[58]

3. THE PAULI ENHANCEMENT FACTOR AND SHELL STRUCTURE

3.1 Representation in Terms of One-Particle Orbitals

Clearly, there is no problem in writing down an exact expression for T_s in terms of orbitals:

$$T_s[\{\phi_i(\mathbf{r})\}] = \frac{1}{2}\sum_{i=1}^{N}\int d^3\mathbf{r}\ \ \nabla_{\mathbf{r}}\phi_i^*(\mathbf{r})\nabla_{\mathbf{r}}\phi_i(\mathbf{r}) \tag{4}$$

Assuming that for atoms the orbitals are products of radial parts times spherical harmonics, namely,

$$\phi_i(\mathbf{r}) = R_i(r)\,Y_{l_i,m_i}(\theta,\varphi) \tag{5}$$

upon angular integration, Eq. (4) adopts the form:

$$T_s[\{R_i(r)\}] = \int dr r^2 \frac{1}{2}\left\{\sum_{i=1}^{N}\left(\frac{dR_i(r)}{dr}\right)^2 + \sum_{i=1}^{N}\frac{l_i(l_i+1)}{r^2}R_i^2(r)\right\} \tag{6}$$

Further, assuming that the one-particle density is averaged over the angular part such that $\rho(\mathbf{r}) \to \rho(r) = \sum_{i=1}^{N} (R_i(r))^2$ and $\nabla_{\mathbf{r}} \rho(\mathbf{r}) = \hat{1}_r \frac{d}{dr} \sum_{i=1}^{N} (R_i(r))^2$, we can rewrite the von Weizsäcker term as:

$$T_W[\{R_i(r)\}] = \frac{1}{2} \int dr r^2 \left\{ \sum_{i=1}^{N} \sum_{j=1}^{N} R_i(r) \frac{dR_i(r)}{dr} R_j(r) \frac{dR_j(r)}{dr} / \sum_{i=1}^{N} (R_i(r))^2 \right\} \tag{7}$$

From Eqs. (6) and (7), after some algebra we can rewrite $T_P = T_s - T_W$ as follows:

$$\begin{aligned} T_P[\{R_i(r)\}] = & \frac{1}{4} \int dr r^2 \frac{1}{\rho(r)} \sum_{i=1}^{N} \sum_{j=1}^{N} \left(R_i(r) \frac{dR_j(r)}{dr} - R_j(r) \frac{dR_i(r)}{dr} \right)^2 \\ & + \frac{1}{2} \int dr r^2 \sum_{i=1}^{N} \frac{l_i(l_i+1)}{r^2} R_i^2(r) \end{aligned} \tag{8}$$

In order to keep the notation similar to that used for local-scaling transformations (LS-DFT, see below)[59] we express the Pauli enhancement factor $F_p[\rho(r);r]$ of Eq. (3), which in this case is a functional of the radial orbitals, as:

$$F_P[\{R_i(r)\}] = (\tau_N[\{R_i(r)\}] + \kappa_N[\{R_i(r)\}]) \tag{9}$$

where

$$\tau_N[\{R_i(r)\}] = \frac{1}{2\rho^{8/3}(r)} \sum_{i=1}^{N-1} \sum_{j=i+1}^{N} W_{ij}[\{R_i(r)\}] \tag{10}$$

$$\kappa_N[\{R_i(r)\}] = \frac{1}{2\rho^{5/3}(r)} \sum_{i=1}^{N} \frac{l_i(l_i+1)}{r^2} R_i^2(r) \tag{11}$$

In Eq. (10) W_{ij} is defined as:

$$W_{ij}[\{R_i(r)\}] = \left(R_i(r) \frac{dR_j(r)}{dr} - R_j(r) \frac{dR_i(r)}{dr} \right)^2 \tag{12}$$

3.1.1 Application to the Al Atom

Aluminum, $Z = 13$ has the following electronic configuration for its ground state: $[1s^2 2s^2 2p^6 3s^2 3p^1]$.

The explicit expression for the modulating factor $\tau_N[\{R_i(r)\}]$ of aluminum is given by

$$\tau_N[\{R_i(r)\}] = \{\tau_{KL} + \tau_{KM} + \tau_{LL} + \tau_{LM} + \tau_{MM}\} \tag{13}$$

where we have collected the terms corresponding to each atomic shell and inter-shell. These terms are defined by

$$\begin{aligned}
\tau_{IJ} &= \frac{1}{2\rho_g^{8/3}(f)}\omega_{IJ} \\
\omega_{KL} &= 4W_{1s2s} + 12W_{1s2p} \\
\omega_{KM} &= 4W_{1s3s} + 2W_{1s3p} \\
\omega_{LL} &= 12W_{2s2p} \\
\omega_{LM} &= 4W_{2s3s} + 2W_{2s3p} + 4W_{2p3s} + 6W_{2p3p} \\
\omega_{MM} &= 2W_{3s3p}
\end{aligned} \tag{14}$$

In what follows we examine in Fig. 1 the behavior of the modulating factor $\tau_N[\{R_i(r)\}]$ for the Al atom by comparing it with the radial distribution $4\pi\, r^2\rho_{HF}(r)$ (τ in the present case is up-scaled by a factor of 20). We observe that the first and second maxima of $\tau[\{R_i(r)\}]$ are placed, respectively, at the first and second minima of the radial distribution. It is clearly seen that these points correspond to the inter-shell boundaries. In the outer region we see that τ grows strongly and approaches infinity thus creating the

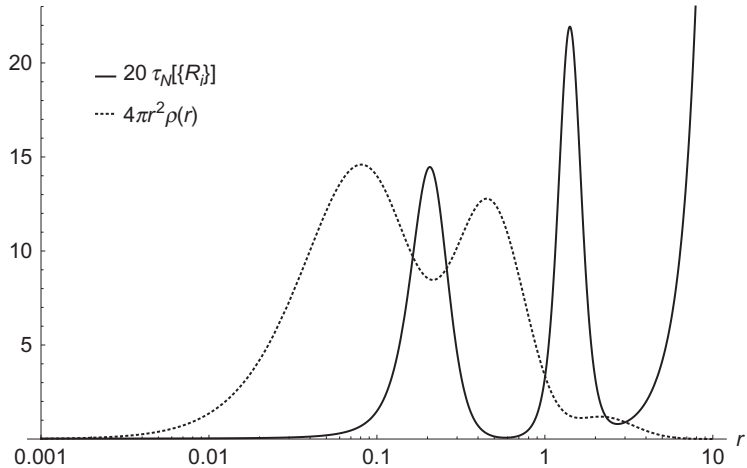

Fig. 1 The full Pauli kinetic energy modulating factor $\tau_N[\{R_i\}]$ for Al (*full line*) calculated by means of Eqs. (13) and (14). The Hartree–Fock radial density of Al is also depicted (*dashed line*).

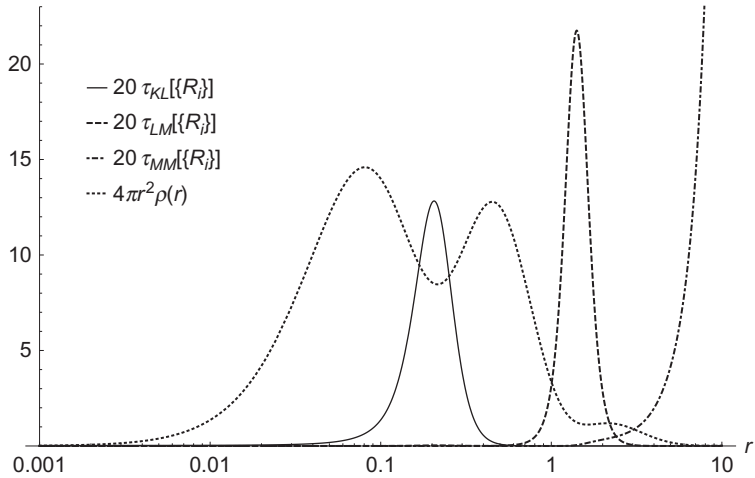

Fig. 2 Graphs of the Pauli kinetic energy modulating factor contributions for Al calculated by means of Eq. (14) for the *KL* and *LM* shell boundaries. The Hartree–Fock radial density of Al is also depicted.

basin that confines electrons to the outer shell. We may infer from Fig. 1 that the Pauli kinetic energy modulating factor bears an important role in the formation of the atomic shells. As seen from this figure, this factor is an essential ingredient for the generation of shell structure in the Al atom. In Fig. 2 we examine the behavior of the different inter-shell components of $\tau[\{R_i(r)\}]$, namely, τ_{KL}, τ_{KL}, and τ_{MM}. It is seen that the first maximum is almost entirely described by τ_{KL}. Similarly, the second one is accounted for by τ_{LM}. The outer border is represented entirely by τ_{MM}. In Fig. 3 we present the separate contribution of τ_{KM} and τ_{LL}. It is clearly seen in Fig. 3 that their contributions are negligible.

3.2 Representation by Means of Local-Scaling Transformations

Although no exact representation of T_s as an explicit functional of the one-particle density has been found so far, López–Boada et al.[59–61] have shown that it is possible to derive an exact albeit implicit form of this functional by resorting to general arguments involving local-scaling transformations. In this derivation, the functional $T_s[\rho]$ takes the form

$$T_s[\rho] = T_W[\rho] + \frac{1}{2}\int d^3\mathbf{r}\rho^{5/3}(\mathbf{r})A_N[\rho(\mathbf{r});\mathbf{r}] \tag{15}$$

where $A_N[\rho(\mathbf{r});\mathbf{r}]$ is an implicit functional of the one-particle density (see later). Note that the von Weizsacker term $T_W[\rho]$, which is an explicit

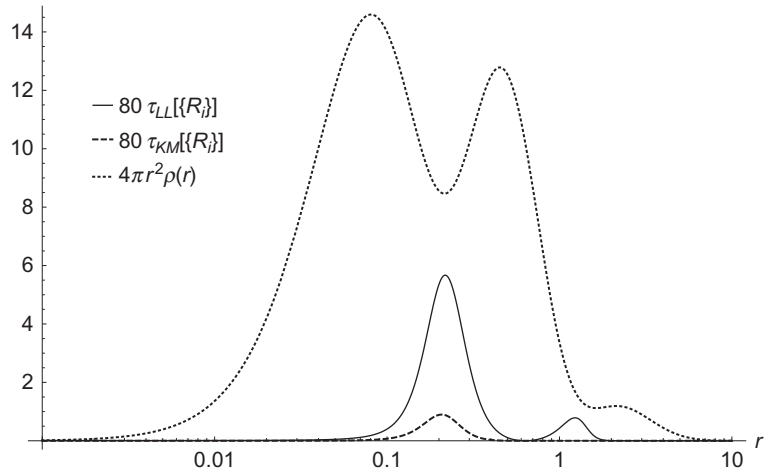

Fig. 3 Graph of the Pauli kinetic energy enhancement factor contribution for Al calculated by means of Eq. (14) for the terms τ_{LL} and τ_{KM} The Hartree–Fock radial density of Al is also depicted.

functional of the one-particle density emerges in a natural fashion in this derivation. The term $A_N[\rho(\mathbf{r}); \mathbf{r}]$ which, except for a numerical factor is equivalent to the Pauli kinetic energy enhancement factor, is however, nonlocal and is closely related to the shell structure of the system. In the case of atoms, for example, $A_N[\rho(\mathbf{r}); \mathbf{r}]$ describes the hills and basins which lead to potentials that localize electrons in shells.

Note that the local-scaling transformation version of density functional theory (LS-DFT)[62–64] is not based on the Hohenberg–Kohn theorems, and thus it is quite different from the Hohenberg–Kohn–Sham version of DFT. LS-DFT is a constructive approach, which allows us to generate energy density functionals that satisfy the variational principle. The ensuing functionals, however, have an implicit dependence on the one-particle density. Local-scaling transformations are coordinate transformations that can be expressed as functions of the one-particle density.[63,65]

A local-scaling transformation carries the vector $\mathbf{r}$ into the vector $\lambda(\mathbf{r})\mathbf{r} \equiv \mathbf{f}$ which has the same direction as $\mathbf{r}$. It can be shown that this transformed vector is $\mathbf{f} \equiv \mathbf{f}([\rho], \mathbf{r})$, namely, it is a function of the one-particle density. As a result, any function which depends on $\mathbf{r}$ may be transformed into another function which depends on $\mathbf{f}([\rho], \mathbf{r})$.

Applying this transformation to the arbitrary "generating" atomic orbital set $\{\phi_{g,i}(\mathbf{r}) = R_{g,i}(r)\, Y_{l_i,m_i}(\theta,\phi)\}_{i=1}^{N}$ one obtains the following set of

transformed orbitals: $\{\phi_{\rho,i}(\mathbf{r}) = R_{\rho,i}(r)\, Y_{l_i,m_i}(\theta,\phi)\}_{i=1}^{N}$ where the locally scaled (density-dependent) radial functions are given by

$$R_{\rho,i}(r) = \sqrt{\frac{\rho(r)}{\rho_g(\lambda(r)r)}}\, R_{g,i}(\lambda(r)r), \tag{16}$$

In Eq. (16) only the radial (or angular-averaged densities) $\rho_g(r) = \sum_{i=1}^{N} |R_{g,i}(r)|^2$ and $\rho(r) = \sum_{i=1}^{N} |R_{\rho,i}(r)|^2$ corresponding to the initial and transformed orbitals, respectively, appear in the expression due to the fact that the vectors maintain the same direction.

A local-scaling transformation relates the densities $\rho(r)$ and $\rho_g(r)$ by means of the following first-order differential equation:

$$\frac{\rho(r)}{\rho_g(\lambda(r)r)} = \lambda(r)^3 \{1 + \mathbf{r}\cdot\nabla_{\mathbf{r}} \ln\, \lambda(r)\} \tag{17}$$

The single Slater determinant Φ_ρ formed from these density-dependent orbitals is

$$\Phi_\rho(\mathbf{r}_1, s_1, \ldots, \mathbf{r}_N, s_N) = \frac{\det}{N!^{1/2}}[\phi_{\rho,1}(\mathbf{r}_1)\sigma_1(s_1)\ldots\, \phi_{\rho,N}(\mathbf{r}_N)\sigma(s_N)] \tag{18}$$

Let us consider now the noninteracting kinetic energy functional given as the expectation value of the kinetic energy operator with respect to the single Slater Φ_ρ:

$$T_s[\Phi_\rho] = \frac{1}{2}\sum_{i=1}^{N}\int_0^\infty dr r^2 \left[\left(\frac{dR_{\rho,i}(r)}{dr}\right)^2 + \frac{l_i(l_i+1)}{r^2}\left(R_{\rho,i}(r)\right)^2\right]. \tag{19}$$

The noninteracting kinetic energy expression given by Eq. (19) is an implicit functional of the one-particle density ρ, namely, $T_s[\Phi_\rho] \equiv T_s[\rho]$ which after some manipulation becomes

$$\begin{aligned} T_s[\rho] = &\frac{1}{8}\int_0^\infty dr\, r^2 \frac{(\nabla\rho(r))^2}{\rho(r)} \\ &+ \int_0^\infty dr\, r^2 \rho^{5/3}(r)\left(1 + \vec{r}\cdot\nabla \ln\, \lambda(r)\right)^{4/3} \tau_N[\rho] \\ &+ \int_0^\infty dr\, r^2 \rho^{5/3}(r)\left(1 + \vec{r}\cdot\nabla \ln\, \lambda(r)\right)^{-2/3} \kappa_N[\rho]. \end{aligned} \tag{20}$$

where the modulating factors $\tau_N[\rho]$ and $\kappa_N[\rho]$ (with $f = \lambda(r)r$) are

$$\tau_N[\rho] = \frac{1}{\rho_g^{8/3}(f)} \frac{1}{2} \sum_{i<j} W_{ij}[\rho] \tag{21}$$

and

$$\kappa_N[\rho] = \frac{1}{\rho_g^{5/3}(f)} \sum_{i=1}^{N} \frac{l_i(l_i+1)}{2} \left(\frac{R_{g,i}(f)}{f} \right)^2, \tag{22}$$

where

$$W_{ij}[\rho] = \left(R_{g,n_i,l_i}(f) \frac{d\, R_{g,n_j,l_j}(f)}{df} - R_{g,n_j,l_j}(f) \frac{d\, R_{g,n_i,l_i}(f)}{df} \right)^2. \tag{23}$$

The Pauli enhancement factor $F_P([\rho]; \mathbf{r})$ is given by

$$\begin{aligned} F_P([\rho]; \mathbf{r}) = & \left(1 + \vec{r} \cdot \nabla \ln \lambda(r)\right)^{4/3} \tau_N \\ & + \left(1 + \vec{r} \cdot \nabla \ln \lambda(r)\right)^{-2/3} \kappa_N \end{aligned} \tag{24}$$

These results have a striking similarity with those given by Eqs. (9), (10), and (11). The difference arises from the presence of density-dependent factors appearing in Eq. (24).

The explicit expression for the modulating factor $\tau[\rho]$ of aluminum is similar to those of Eqs. (13) and (14). It must be kept in mind, however, that in Eq. (24) $\tau[\rho]$ is a functional of the one-particle density and not of the orbitals. The generating orbitals, or broadly speaking, the generating polynomials are functions which depend implicitly on the one-particle density and which change when an approximate ρ evolves toward the exact one. The symmetry of the generating orbitals is the important feature introduced into the local-scaling expression.

In a previous work,[65] the construction of these local-scaling terms was carried out using generalized Slater-type orbitals as the generating one-particle functions. These orbitals are defined by:

$$R_{g,n_j,l_j}(r) \equiv N_{g,n_j,l_j}(f) f_{n_j,l_j}(r) \exp\left(-\alpha_{n_j,l_j} r^{\beta}\right) \tag{25}$$

where $f_{n_j,l_j}(r)$ are orthogonal polynomials.

We refer the reader to Fig. 4 (taken from Ref. 65), where the behavior of the modulating factor $\tau_N[\rho]$ for the Al atom is presented along with the radial distribution $4\pi\, r^2 \rho_{HF}(r)$. Note that $\tau[\rho]$ has been down-scaled by a factor of 200 in view of the fact that $\tau[\{R_i\}]$ and $\tau[\rho]$ differ by a factor (see Eq. 13). We observe, however, that as in the case for $\tau[\{R_i\}]$ the first and second maxima

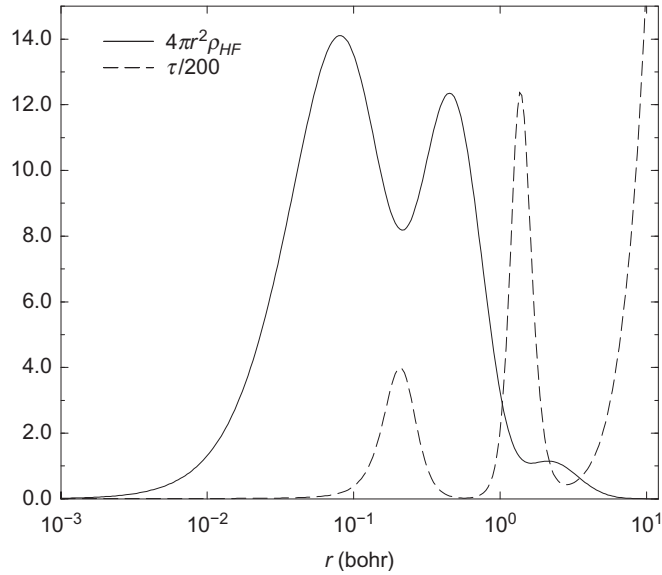

Fig. 4 The full Pauli kinetic energy modulating factor $\tau_N[\rho]$ for Al (*dashed line*) calculated by local-scaling transformations. The Hartree–Fock radial density of Al is also depicted (*full line*). *From Ludeña, E. V.; Karasiev, V.; López-Boada, R.; Valderrama, E.; Maldonado, J. Local-Scaling Transformation Version of Density Functional Theory: Application to Atoms and Diatomic Molecules.* J. Comput. Chem. ***1999,*** 20 *(1), 155–183.*

are placed, respectively, at the first and second minima of the radial distribution. Moreover, the tail behavior of this graph resembles that of the previous case in that it goes to infinity for large r. In Fig. 5, a detailed graph depicting the behavior of τ_{KL} and τ_{LM} is presented. Finally, in Fig. 6, the individual behavior of the terms τ_{KM}, τ_{LL}, and τ_{LM} is plotted.

3.3 The Explicit Functional Representation for T_p in Terms of the Liu–Parr Expansion

In recent work[66] we have applied the Liu and Parr[67] power series expansion originally used for the noninteracting kinetic energy functional T_s to represent, in the present case, the Pauli kinetic energy functional:

$$T_p[\rho] = \sum_{j=1}^{n} C_j \left[\int d^3\mathbf{r} \rho^{[1+2/3j]}(\mathbf{r}) \right]^j \tag{26}$$

It follows from this expression that the Pauli enhancement factor is given by

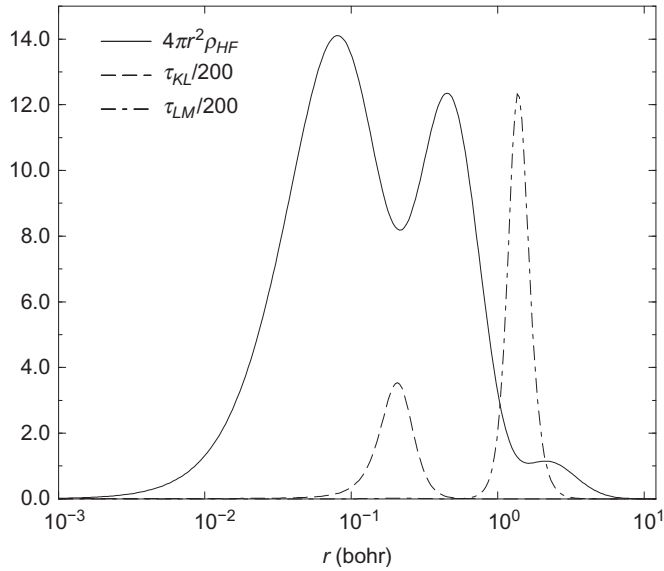

Fig. 5 Graphs of the Pauli kinetic energy modulating factor contributions for Al (*dashed line*) calculated by local-scaling transformations corresponding to the *KL* and *LM* shell boundaries. The Hartree–Fock radial density of Al is also depicted (*full line*). *From Ludeña, E. V.; Karasiev, V.; López-Boada, R.; Valderrama, E.; Maldonado, J. Local-Scaling Transformation Version of Density Functional Theory: Application to Atoms and Diatomic Molecules.* J. Comput. Chem. ***1999,*** 20 *(1), 155–183.*

$$F_p[\rho(\mathbf{r});\mathbf{r}] = \sum_{j=1}^{n} C_j \rho^{(2/3)(1/j-1)}(\mathbf{r}) \left[\int d^3\mathbf{r}\rho^{[1+2/3j]}(\mathbf{r})\right]^{j-1} \tag{27}$$

The justification for applying the Liu–Parr expansion to the kinetic energy functional T_p is that upon simple coordinate scaling T_s given by Eq. (4) scales as $T_s^{\lambda} = \lambda^2 T_s$. Similarly, the von Weizsäcker term also scales as $T_W^{\lambda} = \lambda^2 T_W$. It follows that $T_p^{\lambda} = \lambda^2 T_p$. Hence, the application of the Liu–Parr expansion to T_P is justified.

In the original Liu–Parr expansion for T_s the coefficients were fixed by an optimal least-square fit to the "exact," Hartree–Fock values for atoms from H to Kr. The aptness of this expansion to represent adequately the shell structure of atoms was examined recently.[68] By and large, the three-term expansion of Liu and Parr reproduces the shape of the enhancement factor of the atoms considered quite closely, provided that a local contribution $\nu\nabla^2\rho(\mathbf{f})$ (where ν is a parameter) is added. Notice that the addition of this term does not contribute to the energy. The three-term Liu–Parr expansion, however, does not lead to satisfactory values of the

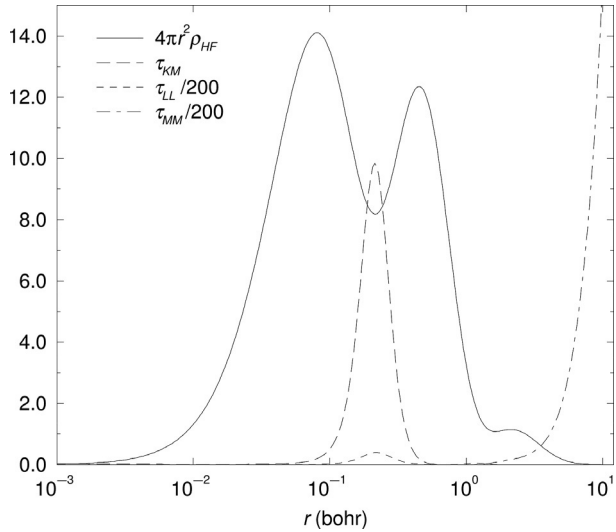

Fig. 6 Graph of the Pauli kinetic energy enhancement factor contribution for Al (*dashed line*) calculated by local-scaling transformations corresponding to the *KM*, *LL*, and *MM* terms. The Hartree–Fock radial density of Al is also depicted (*full line*). *From Ludeña, E. V.; Karasiev, V.; López-Boada, R.; Valderrama, E.; Maldonado, J. Local-Scaling Transformation Version of Density Functional Theory: Application to Atoms and Diatomic Molecules.* J. Comput. Chem. ***1999,*** 20 *(1), 155–183.*

noninteracting kinetic energy T_s for the thirty six atoms examined going from H to Kr.[68]

In Fig. 7, we present the enhancement factor $F_p[\rho]$ calculated for the Liu–Parr expansion with $n = 7$. We also present graphs for the radial distribution and for the Hartree–Fock approximation to the enhancement term $\tau[\{R_i\}]$. It is seen from Fig. 7 that the form of the enhancement factor for the aluminum atom, when it is calculated via the shell-by-shell optimization, is broadly located in the region where $\tau_{LM}[\{R_i\}]$ has its maximum. The fit is even looser when the factor uses the all-shell optimized coefficients.

In Table 1 we present the results of the Liu–Parr expansion for the noninteracting kinetic energies $T_s[\rho]$ and the Pauli kinetic energy $T_p[\rho]$. It is seen from this table that the approximations to the exact Hartree–Fock values of these quantities is very close such that the errors are $\Delta T_s = 0.0064$ Hartrees and $\Delta T_p = 0.0130$ Hartrees, respectively. These values correspond to the best approximation obtained to date. The fact that the enhancement factor does not perfectly fit the exact form given by the Hartree–Fock functional indicates that in the optimization process carried shell-by-shell the function adapted itself as much as possible to reproduce the form of $\tau_{LM}[\{R_i\}]$.

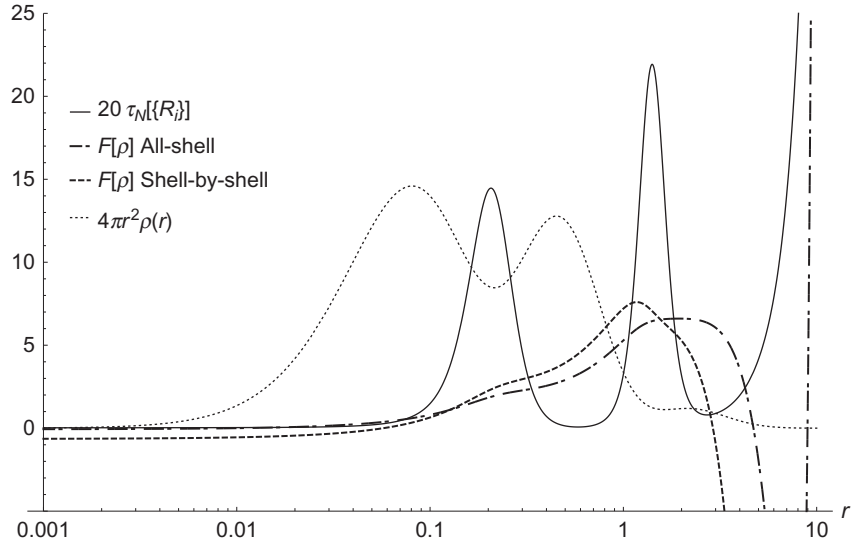

Fig. 7 The Pauli kinetic energy modulating factor $F_p[\rho]$ for Al corresponding the Liu–Parr power series expansion for $n = 7$ evaluated with all-shell and shell-by-shell optimized coefficients. The Hartree–Fock radial density $\tau[\{R_i\}]$ of Al is also depicted.

Table 1 Noninteracting Kinetic Energy Values T_s and Pauli Kinetic Energy Values T_p (in Hartrees) for the Liu–Parr Power Series Approximations With All-Shells and Shell-by-Shell Coefficient Optimization for the Aluminum Atom

n	T_s^{HF}	T_s^{app}[a]	T_p^{app}[b]	T_p^{HF}	T_p^{app}[a]	T_p^{app}[b]
3	241.8720	245.9413	241.7640	85.1129	89.1755	84.9982
4	241.8720	241.7826	241.8630	85.1129	85.0169	85.0976
5	241.8720	241.6821	241.8240	85.1129	84.9163	85.0578
6	241.8720	241.4830	241.6767	85.1129	84.7166	85.1010
7	241.8720	241.8686	241.8656	85.1129	85.1029	85.0999

[a]All-shells.
[b]Shell-by-shell.
For comparison the respective Hartree–Fock values are included.

4. DISCUSSION

We have examined in the present work the various approximations to the Pauli enhancement factors which may be obtained by means of orbital representations, local-scaling representations, and Liu–Parr power series

expansions and have related them to the appearance of shell structure in atoms. We have taken as a working example the aluminum atom.

The relation of an orbital representation with shell structure can be established in a direct fashion. Orbitals carry in them the symmetry which allows for an exact description of shell structure. This is the reason why calculation based on orbitals such as Hartree–Fock of Kohn–Sham DFT lead to the correct inclusion of shell structure. On the other hand, when we want to do away with orbitals and construct kinetic energy functionals which depend on the one-particle density, it is seen that the result is not at all obvious. It depends on the way the functional is constructed. For example, when we use generating orbitals having the correct orthogonality conditions, such as in the LS-DFT application discussed in this work, the resulting functionals (which are implicit functional of the one-particle density) maintain the shell structure characteristics as the original orbital ones. Thus, in this case, shell structure is incorporated in the functionals through the symmetry properties of the generating orbitals.

The problem at hand is, however, how to construct explicit functionals of the one-particle density which nevertheless keep the shell structure traits of the exact functionals. It is seen that through the use of the Liu–Parr power series expansions, this aim is only partially fulfilled. The shell-by-shell optimization leads to excellent values of the $T_s[\rho]$ and $T_p[\rho]$ functionals. However, the sharp curves denoting shell structure are not totally defined. The present results show that there is still much work to be done in the endeavor of obtaining both accurate and shell-structure-reproducing functionals.

ACKNOWLEDGMENTS

E.V.L. would like to gratefully acknowledge financial support to CIDNA from ESPOL authorities. E.X.S. is grateful to EACEA for allowing him to be part of the Erasmus Mundus Joint Master Degree Theoretical Chemistry and Computational Modelling (TCCM).

REFERENCES

1. Romera, E.; Dehesa, J. S.; Yánez, R. J. The Weizsäcker Functional: Some Rigorous Results. *Int. J. Quantum Chem.* **1995**, *56*(5), 627–632.
2. Romera, E.; Sánchez-Moreno, P.; Dehesa, J. S. The Fisher Information of Single-Particle Systems With a Central Potential. *Chem. Phys. Lett.* **2005**, *414*(4), 468–472.
3. Bohórquez, H. J.; Boyd, R. J. On the Local Representation of the Electronic Momentum Operator in Atomic Systems. *J. Chem. Phys.* **2008**, *129*(2), 024110.
4. Anderson, J. S.; Ayers, P. W. Hernandez, J. I. R.. How Ambiguous is the Local Kinetic Energy?*J. Phys. Chem. A* **2010**, *114*(33), 8884–8895.
5. Ludeña, E. V. On the Nature of the Correction to the Weizsäcker Term. *J. Chem. Phys.* **1982**, *76*(6), 3157–3160.

6. Pauling, L. The Theoretical Prediction of the Physical Properties of Many-Electron Atoms and Ions. Mole Refraction, Diamagnetic Susceptibility and Extension in Space. *Proc. R. Soc. A* **1927**, *114*, 181–211.
7. Pauli, W. Uber den Zusammenhang des Abschlusses der Elektronengruppen im Atom mit der Komplexstruktur der Spektren. *Z. Phys.* **1925**, *31*, 765.
8. Pauli, W. Exclusion Principle and Quantum Mechanics. 1946. Nobel Lecture.
9. Schrödinger, E. Quantisierung als Eigenwertproblem. *Ann. Phys.* **1926**, *385*(13), 437–490.
10. Ünsold, A. Beiträge zur Quantenmechanik der Atome. *Ann. Phys.* **1927**, *387*, 355–393.
11. Slater, J. C. Atomic Shielding Constants. *Phys. Rev.* **1930**, *36*, 57–64.
12. Bartell, L. S.; Brockway, L. O. Electron Diffraction Study of the Structure of Trimethylphosphine. *J. Chem. Phys.* **1960**, *32*(2), 512–515.
13. Weinstein, H.; Politzer, P.; Srebrenik, S. A Misconception Concerning the Electronic Density Distribution of an Atom. *Theoret. Chim. Acta* **1975**, *38*(2), 159–163.
14. Angulo, J. C.; Dehesa, J. S. Atomic Systems With a Completely Monotonic Electron Density. *Phys. Rev. A* **1991**, *44*(3), 1516.
15. Wang, W. P.; Parr, R. G. Statistical Atomic Models With Piecewise Exponentially Decaying Electron Densities. *Phys. Rev. A* **1977**, *16*, 891–902.
16. Hoffmann-Ostenhof, T.; Hoffmann-Ostenhof, M.; Ahlrichs, R. Schrödinger Inequalities and Asymptotic Behavior of Many-Electron Densities. *Phys. Rev. A* **1978**, *18*(2), 328.
17. Hoffmann-Ostenhof, M.; Thirring, W.; Hoffmann-Ostenhof, T. Simple Bounds to the Atomic One-Electron density at the Nucleus and to Expectation Values of One-Electron Operators. *J. Phys. B: At. Mol. Phys.* **1978**, *11*(19), L571.
18. Vidal, J. P.; Vidal-Valat, G.; Galtier, M.; Kurki-Suonio, K. X-Ray Study of the Charge Distribution in MgF2. *Acta Crystallogr. Sect. A: Cryst. Phys. Diffr. Theor. Gen. Crystallogr.* **1981**, *37*(6), 826–837.
19. Simas, A. M.; Sagar, R. P.; Ku, A. C. Smith, V. H., Jr. The Radial Charge Distribution and the Shell Structure of Atoms and Ions. *Can. J. Chem.* **1988**, *66*(8), 1923–1930.
20. Sagar, R. P.; Ku, A. C.; Smith, V. H., Jr. An Examination of the Shell Structure of Atoms and Ions as Revealed by the One-Electron Potential. *Can. J. Chem.* **1988**, *66*(4), 1005–1012.
21. Angulo, J. C.; Dehesa, J. S.; Gálvez, F. J. Atomic-Charge Convexity and the Electron Density at the Nucleus. *Phys. Rev. A* **1990**, *42*(1), 641.
22. Esquivel, R. O.; Sagar, R. P.; Smith, V. H., Jr.. Chen, J.; Stott, M. J. Pseudoconvexity of the Atomic Electron Density: A Numerical Study. *Phys. Rev. A* **1993**, *47*(6), 4735.
23. Esquivel, R. O.; Chen, J.; Stott, M. J.; Sagar, R. P. Smith, V. H., Jr.. Pseudoconvexity of the Atomic Electron Density: Lower and Upper Bounds. *Phys. Rev. A* **1993**, *47*(2), 936.
24. Kohout, M.; Savin, A.; Preuss, H. Contribution to the Electron Distribution Analysis. I. Shell Structure of Atoms. *J. Chem. Phys.* **1991**, *95*(3), 1928–1942.
25. Schmider, H.; Sagar, R. P. Smith, V. H., Jr.. Does the Atomic Structure Factor Show Atomic Structure?*J. Chem. Phys.* **1991**, *94*(6), 4346–4351.
26. Schmider, H.; Sagar, R. P. Smith, V. H., Jr.. An Investigation of Atomic Structure in Position and Momentum Space by Means of "ideal shells"*Can. J. Chem.* **1992**, *70*(2), 506–512.
27. Parr, R. G.; Zhou, Z. Absolute Hardness: Unifying Concept for Identifying Shells and Subshells in Nuclei, Atoms, Molecules and Metallic Clusters. *Acc. Chem. Res.* **1993**, *26*, 256–258.
28. Aptekarev, A. I.; Dehesa, J. S.; Yáñez, R. J. Spatial Entropy of Central Potentials and Strong Asymptotics of Orthogonal Polynomials. *J. Math. Phys.* **1994**, *35*(9), 4423–4428.
29. Yáñez, R. J.; Angulo, J. C.; Dehesa, J. S. Information Entropies of Many-Electron Systems. *Int. J. Quantum Chem.* **1995**, *56*(5), 489–498.

30. Angulo, J. C.; Antolín, J.; Sen, K. D. Fisher-Shannon Plane and Statistical Complexity of Atoms. *Phys. Lett. A* **2008**, *372*(5), 670–674.
31. Guerrero, A.; Sánchez-Moreno, P.; Dehesa, J. S. Upper Bounds on Quantum Uncertainty Products and Complexity Measures. *Phys. Rev. A* **2011**, *84*(4), 042105.
32. Jesus, S. D.; Martinez-Finkelshtein, A.; Sánchez-Ruiz, J. Quantum Information Entropies and Orthogonal Polynomials. *J. Comput. Appl. Math.* **2001**, *133*, 23–46.
33. Dehesa, J. S.; Martínez-Finkelshtein, A.; Sorokin, V. N. Information-Theoretic Measures for Morse and PöschlTeller Potentials. *Mol. Phys.* **2006**, *104*(4), 613–622.
34. López-Rosa, S.; Angulo, J. C.; Dehesa, J. S. Spreading Measures of Information-Extremizer Distributions: Applications to Atomic Electron Densities in Position and Momentum Spaces. *Eur. Phys. J. D* **2009**, *51*(3), 321–329.
35. Fricke, M.; Lorke, A.; Kotthaus, J. P.; Medeiros-Ribeiro, G.; Petroff, P. M. Shell Structure and Electron-Electron Interaction in Self-Assembled InAs Quantum Dots. *Europhys. Lett.* **1996**, *36*(3), 197.
36. Yanson, A. I.; Yanson, I. K.; van Ruitenbeek, J. M. Observation of Shell Structure in Sodium Nanowires. *Nature* **1999**, *400*(6740), 144–146.
37. Kohout, M.; Savin, A. Atomic Shell Structure and Electron Numbers. *Int. J. Quantum Chem.* **1996**, *60*(4), 875–882.
38. Sen, K. D.; Gayatri, T. V.; Toufar, H. Shell Structure of Atoms. *J. Mol. Struct. (THEOCHEM)* **1996**, *361*(1), 1–13.
39. Bohórquez, H. J.; Boyd, R. J. A Localized Electrons Detector for Atomic and Molecular Systems. *Theor. Chem. Acc.* **2010**, *127*(4), 393–400.
40. Bohórquez, H. J.; Matta, C. F.; Boyd, R. J. The Localized Electrons Detector as an Ab Initio Representation of Molecular Structures. *Int. J. Quantum Chem.* **2010**, *110*(13), 2418–2425.
41. Bohórquez, H. J.; Boyd, R. J.; Matta, C. F. Molecular Model With Quantum Mechanical Bonding Information. *J. Phys. Chem. A* **2011**, *115*(45), 12991–12997.
42. Finzel, K.; Kohout, M. How Does the Ambiguity of the Electronic Stress Tensor Influence Its Ability to Reveal the Atomic Shell Structure. *Theor. Chem. Acc.* **2013**, *132*(11), 1–13.
43. Finzel, K. Shell-Structure-Based Functionals for the Kinetic Energy. *Theor. Chem. Acc.* **2015**, *134*(9), 106.
44. Finzel, K. A Simple Approximation for the Pauli Potential Yielding Self-Consistent Electron Densities Exhibiting Proper Atomic Shell Structure. *Int. J. Quantum Chem.* **2015**, *115*(23), 1629–1634.
45. Finzel, K. Reinvestigation of the Ideal Atomic Shell Structure and Its Application in Orbital-Free Density Functional Theory. *Theor. Chem. Acc.* **2016**, *135*(4), 1–6.
46. Finzel, K. Local Conditions for the Pauli Potential in Order to yield Self-Consistent Electron Densities Exhibiting Proper Atomic Shell Structure. *J. Chem. Phys.* **2016**, *144*(3), 034108.
47. Finzel, K. Approximating the Pauli Potential in Bound Coulomb Systems. *Int. J. Quantum Chem.* **2016**, *116*(16), 1261–1266.
48. March, N. H.; Murray, A. M. Electronic Wave Functions Round a Vacancy in a Metal. *Proc. R. Soc. Lond. A Math. Phys. Sci* **1960**, *256*(1286), 400–415.
49. Levy, M.; Perdew, J. P.; Sahni, V. Exact Differential Equation for the Density and Ionization Energy of a Many-Particle System. *Phys. Rev. A* **1984**, *30*(5), 2745.
50. March, N. H. Differential Equation for the Ground-State Density in Finite and Extended Inhomogeneous Electron Gases. *Phys. Lett. A* **1985**, *113*(2), 66–68.
51. March, N. H. The Local Potential Determining the Square Root of the Ground-State Electron Density of Atoms and Molecules From the Schrödinger Equation. *Phys. Lett. A* **1986**, *113*(9), 476–478.

52. Kryachko, E. S.; Ludeña, E. V. Formulation of *N*-and *v*-Representable Density functional Theory V. Exchange Only Self-Consistent Field. *Int. J. Quantum chem.* **1992**, *43*(6), 769–782.
53. Levy, M.; Görling, A. Recent Constrained-Search Advances for Approximating Density Functionals. *Philos. Mag. B* **1994**, *69*(5), 763–769.
54. March, N. H. The Pauli Potential in Relation to the Differential Virial Theorem With Application to Experiments on Ultracold Atomic Gases of Fermions. *Phys. Lett. A* **2008**, *372*(44), 6667–6669.
55. March, N. H. Concept of the Pauli Potential in Density Functional Theory. *J. Mol. Struct.: THEOCHEM* **2010**, *943*(1), 77–82.
56. Levämäki, H.; Nagy, A.; Kokko, K.; Vitos, L. Cusp Relation for the Pauli Potential. *Phys. Rev. A* **2014**, *90*(6), 062515.
57. Piris, M.; March, N. H. Is the Hartree-Fock Prediction that the Chemical Potential μ of Non-Relativistic Neutral Atoms is Equal to Minus the Ionisation Potential I Sensitive to Electron Correlation? *Phys. Chem. Liq.* **2015**, *53*(6), 696–705.
58. Levämäki, H.; Nagy, A.; Kokko, K.; Vitos, L. Alternative to the Kohn-Sham Equations: The Pauli Potential Differential Equation. *Phys. Rev. A* **2015**, *92*(6), 062502.
59. López-Boada, R.; Ludeña, E. V.; Karasiev, V.; Colle, R. Generation of Explicit Electron Correlation Functional by Means of Local Scaling Transformations. *Int. J. Quantum Chem.* **1998**, *69*(4), 439–450.
60. López-Boada, R.; Ludeña, E. V. Hartree-Fock Calculations in the Context of the Local-Scaling Transformation Version of Density Functional Theory. Applications to the Lithium and Beryllium Atoms. *Int. J. Quantum Chem.* **1998**, *96*, 485.
61. López-Boada, R.; Karasiev, V.; Ludeña, E. V.; Colle, R. Atomic Kinetic and Exchange Energy Functionals by Means of Local-Scaling Transformations. *Int. J. Quantum Chem.* **1998**, *69*(4), 503–512.
62. Kryachko, E. S.; Ludeña, E. V. L. *Energy Density Functional Theory of Many-Electron Systems*. Kluwer Academic Publishers: Dordrecht, 1990.
63. Kryachko, E. S.; Ludeña, E. V. Formulation of *N*-and *v*-Representable Density-Functional Theory. I. Ground States. *Phys. Rev. A* **1991**, *43*(5), 2179.
64. Kryachko, E. S.; Ludeña, E. V. Density Functional Theory: Foundations Reviewed. *Phys. Rep.* **2014**, *544*(2), 123–239.
65. Ludeña, E. V.; Karasiev, V.; López-Boada, R.; Valderrama, E.; Maldonado, J. Local-Scaling Transformation Version of Density Functional Theory: Application to Atoms and Diatomic Molecules. *J. Comput. Chem.* **1999**, *20*(1), 155–183.
66. Ludeña, E. V.; Salazar, E. X.; Cornejo, M. H.; Arroyo, D. E.; Karasiev, V. V. Representation of the Pauli Kinetic Energy Functional in Terms of the Liu-Parr Power Series Expansion: Application to Atoms. *Phys. Rev. A* **2017**, (submitted for publication).
67. Liu, S.; Parr, R. G. Expansions of Density Functionals in Terms of Homogeneous Functionals: Justification and Nonlocal Representation of the Kinetic Energy, Exchange Energy, and Classical Coulomb Repulsion Energy for Atoms. *Phys. Rev. A* **1997**, *55*, 1792.
68. Salazar, E. X.; Guarderas, P. F.; Ludeña, E. V.; Cornejo, M. H.; Karasiev, V. V. Study of Some Simple Approximations to the Noninteracting Kinetic Energy Functional. *Int. J. Quantum Chem.* **2016**, *116*(17), 1313–1321.